

## Efficient and flexible approach to ptychography using an optimization framework based on automatic differentiation: supplement

JACOB SEIFERT,<sup>1,\*</sup>  DORIAN BOUCHET,<sup>1</sup>  LARS LOETGERING,<sup>2</sup>   
AND ALLARD P. MOSK<sup>1</sup> 

<sup>1</sup>*Nanophotonics, Debye Institute for Nanomaterials Science and Center for Extreme Matter and Emergent Phenomena, Utrecht University, P. O. Box 80000, 3508 TA Utrecht, The Netherlands*

<sup>2</sup>*Advanced Research Center for Nanolithography, Science Park 106, 1098 XG Amsterdam, The Netherlands*  
*\*j.seifert@uu.nl*

---

This supplement published with The Optical Society on 8 January 2021 by The Authors under the terms of the [Creative Commons Attribution 4.0 License](https://creativecommons.org/licenses/by/4.0/) in the format provided by the authors and unedited. Further distribution of this work must maintain attribution to the author(s) and the published article's title, journal citation, and DOI.

Supplement DOI: <https://doi.org/10.6084/m9.figshare.13325738>

Parent Article DOI: <https://doi.org/10.1364/OSAC.411174>

# Efficient and flexible approach to ptychography using an optimization framework based on automatic differentiation: supplemental document

This document provides supplementary information to “Efficient and flexible approach to ptychography using an optimization framework based on automatic differentiation”.

## 1. AMPLITUDE AND PHASE CORRELATIONS

Correlating the ground truth with the reconstructed complex-valued object using equation (4) provides an accurate measure of the overall reconstruction performance. To gain knowledge about the reconstruction performance of the amplitude and phase images independently, it is useful to correlate them to the ground truth separately. Since the phase values in ptychography are cyclic variables and not absolute, one has to avoid spurious influences from phase wrapping and global phase shift when comparing two phase images. This is achieved by computing the magnitude of the complex correlation of  $\exp[i\varphi(\mathbf{r})]$ , where  $\varphi(\mathbf{r}) = \arg[O(\mathbf{r})]$  represents the phase image. The results are shown in Fig. S1.

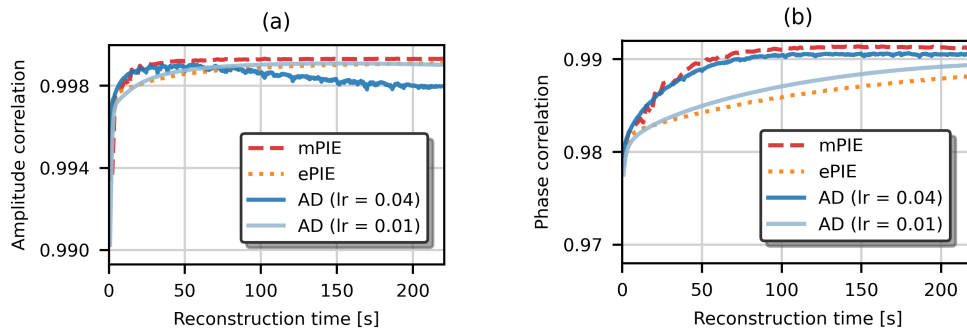


**Fig. S1.** Convergence results for reconstructions using mPIE, ePIE and our AD-based framework in simulation for (a) amplitude images and (b) phase images. The correlations between the ground truth and the reconstruction estimates are shown as a function of computation time. All algorithms run on the same computer hardware. lr: learning rate for the Adam optimizer.

## 2. DIFFRACTION INTENSITIES AND SCANNING TRAJECTORIES

In Fig. S2, a selection of randomly selected diffraction intensities for both the synthetic and experimental ptychography datasets are shown. The diffraction intensities are shown after the application of Poisson noise and readout noise, and are sampled with a dynamic range of 12 bits. Furthermore, the scanning trajectories for the probe positions are visualized in Fig. S3. To avoid the raster grid pathology in ptychography, we utilize trajectories following a concentric pattern for the experiment and Poisson disk sampling for the synthetic data [1, 2].

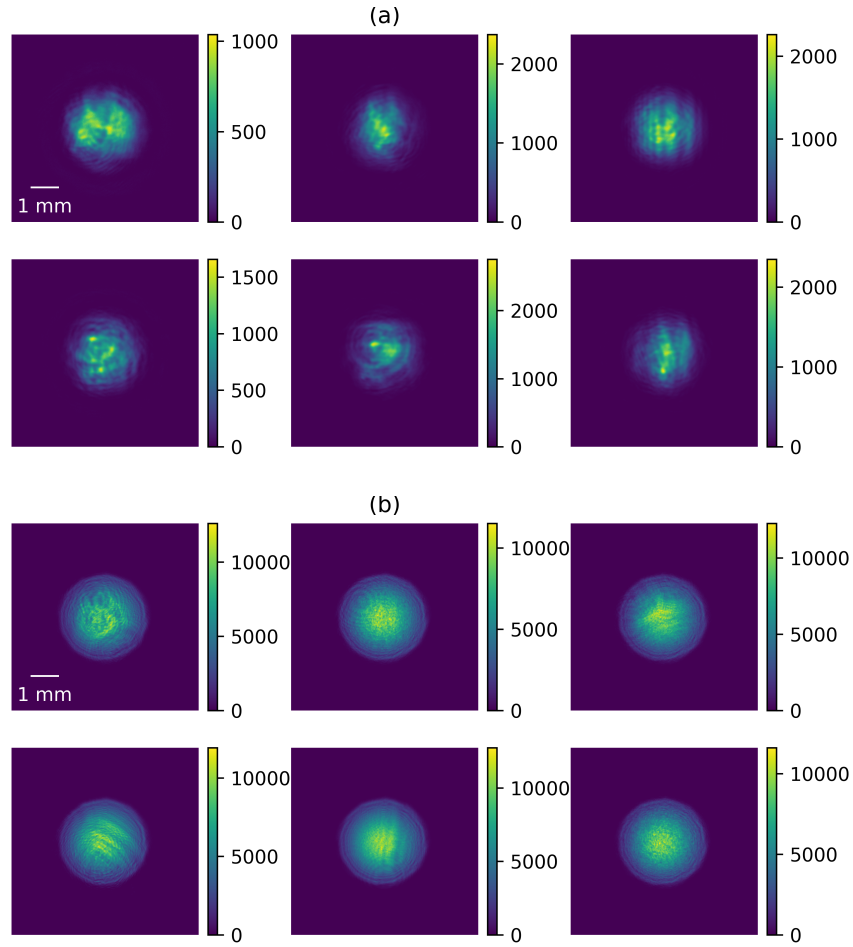


**Fig. S2.** Random selection of diffraction intensities used for phase retrieval. (a) Synthetic data and (b) experimental data. The colorbars denote the counts of the photoelectric detector.

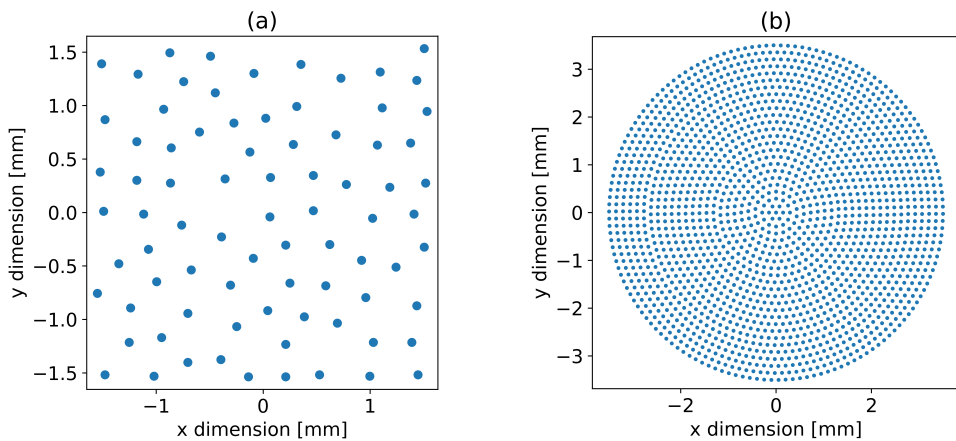


**Fig. S3.** Scanning trajectories for the probe positions used to illuminate the object. (a) Synthetic data with a total of 80 positions and (b) experimental data with a total of 1824 positions.

### 3. RECONSTRUCTION OF A RESOLUTION TEST SAMPLE

A quantitative assessment of the resolution in a biological specimen is difficult. Fourier ring correlation (FRC) is an unbiased and general method to measure the degree of correlation of the two images at different spatial frequencies. Despite it being promising, we have observed that FRC can produce spurious correlations in ptychography, making it hard to interpret the results. Therefore, we are falling back to the reliable approach of imaging a sector star test sample. Subsequently, we can compare the achieved resolutions from reconstructing the data set using both mPIE and our AD-based framework. The experimental setup is identical to the one used for the reconstruction of the mouse cerebellum and shown in Fig. 5 in the main document. Only the object-camera distance has been changed from 34.95 mm to 46.87 mm. The reconstructed transmittances are shown in Fig. S4. The inner center circle of the sector star has a diameter of 200  $\mu\text{m}$  and a total of 72 lines, resulting in a density of 115 lines per mm at the center circle or a line width of 8.7  $\mu\text{m}$ . It should be noted that both reconstructions do not entirely resolve the very finest details of the sector star, indicating an achieved effective resolution of roughly 10  $\mu\text{m}$ . No significant difference between mPIE and our AD-based reconstruction is present. Note that the diffraction limit of the optical system with the given object-camera distance and detector size is approximately 3  $\mu\text{m}$ .

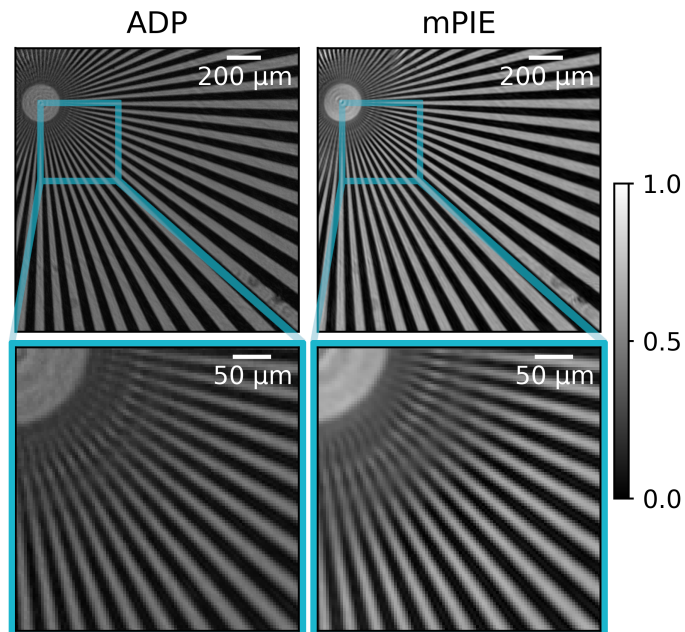


**Fig. S4.** Reconstruction results from experimental data. The transmittance contrast of a sector star is reconstructed using our AD-based framework and mPIE.

### REFERENCES

1. X. Huang, H. Yan, R. Harder, Y. Hwu, I. K. Robinson, and Y. S. Chu, "Optimization of overlap uniformness for ptychography," *Opt. Express* **22**, 12634–12644 (2014).
2. R. Bridson, "Fast poisson disk sampling in arbitrary dimensions," *SIGGRAPH sketches* **10**, 1 (2007).